J Therm Anal Calorim (2015) 119:425–433
DOI 10.1007/s10973-014-4195-3

Using the Friedman method to study the thermal degradation kinetics of photonically cured electrically conductive adhesives

Hui-Wang Cui · Jin-Ting Jiu · Tohru Sugahara · Shijo Nagao · Katsuaki Suganuma · Hiroshi Uchida · Kurt A. Schroder

Received: 4 March 2014 / Accepted: 21 September 2014 / Published online: 1 October 2014

Abstract In this study, the electrically conductive adhesives were fabricated using vinyl ester resin and micro silver flakes, and then a high-intensity pulsed light was introduced to cure the adhesives under an ambient atmosphere at room temperature. The thermal degradation kinetics of photonically cured products was studied using the Friedman method and deduced by assuming a variable activation energy (E). The value of E spanned from 110 to 233 kJ mol^{-1}, which first increased, then decreased, and finally increased again as the thermal degradation proceeded. The kinetic equation of thermal degradation was obtained as $d\alpha/dt = e^{26.62}(1-\alpha)^{2.22}\alpha^{1.85}e^{(-E(\alpha)/RT)}$ with $E(\alpha) = 961.73\alpha^3 - 1453.9\alpha^2 + 669.79\alpha + 79.859$, $\alpha \in (0, 1)$, where α was the fractional extent conversion at a given time (or given temperature). The overall order of reaction was 4.07 and >1, demonstrating that the thermal degradation was complex. With the Friedman method, a comprehensive and in-depth understanding of the thermal degradation kinetics of photonically cured electrically conductive adhesives has been achieved.

Keywords Electrically conductive adhesives · Friedman method · Thermal degradation · Kinetics · Photonic curing

H.-W. Cui (✉) · J.-T. Jiu · T. Sugahara · S. Nagao · K. Suganuma
Institute of Scientific and Industrial Research, Osaka University, Mihogaoka 8-1, Osaka, Ibaraki 567-0047, Japan
e-mail: cuihuiwang@hotmail.com

H. Uchida
Institute for Polymers and Chemicals Business Development Center, Showa Denko K. K., 5-1 Yawata Kaigan Dori, Ichihara, Chiba 290-0067, Japan

K. A. Schroder
NCC Nano, LLC, 400 Parker Drive, Suite 1110, Austin, TX 78728, USA

Introduction

Electrically conductive adhesives (ECAs) are green electronic connecting materials and are often used in special applications which require high temperatures, such as ceramic substrates, thick film circuits, GPS ceramic antennas, buzzers, thick film heaters, chip components, ozone generators, etc. [1–3]. These ECAs are required to possess good high temperature stability. The cured products should be able to bear short-term high temperatures around 350 °C in hot-press leading, long-term high temperatures at 150–170 °C, and above 200 °C, in storage assessments [1–3]. Therefore, functional resins, e.g., epoxy [4–6], silicone resin [7, 8], polyimide resin [9, 10], phenol-formaldehyde resin [11, 12], polyurethane [13, 14], and acrylic resin [15, 16], and functional fillers, e.g., copper particles [17, 18], micro silver flakes [19, 20], nano silver rods [21, 22], functionalized carbon nanotubes [23–25], silver-plated nano graphite sheets [26, 27], nano silver wires [28, 29], and nano hexagonal boron nitride particles [30–32], have been developed to improve the thermal conductivity and thermal resistance. Most of these ECAs are cured by heat in 30–60 min at 120–150 °C or by ultraviolet rays in several to tens of minutes.

In a previous study [33], the ECAs were fabricated using vinyl ester resin and micro silver flakes, and a series of high-intensity pulsed light from a Xenon flash lamp was used to cure the adhesives under ambient atmosphere at room temperature. The ECAs absorbed the intensity pulsed light, which initialized the double bonds in the resin to achieve crosslinking and curing. The photonic curing could be finished within a second under ambient atmosphere at room temperature over a large area. A typical curing time was 140 ms. The ECAs had low bulk resistivity (e.g., 7.54×10^{-6} Ω cm), high bonding strength (e.g.,

6.75 MPa), and high thermal decomposition temperatures above 350 °C. However, the thermal degradation kinetics was not involved in the previous study. In order to clearly understand the reaction mechanism, the thermal degradation kinetics of the adhesive after photonic curing was attempted to study. To obtain the kinetics, the reaction mechanism, activation energy (E), and pre-exponential factor (A) should be determined by using thermal analysis techniques to study the physical changes or chemical reactions. The kinetics has important significances: in theory, it can be used to investigate the reaction mechanism of physical changes and chemical reactions, especially for heterogeneous and non-isothermal reactions; in production, it can provide design parameters for reactors; in application, it can be used to build the relationships among progress, time, and temperature, predict the shelf life for materials and products, estimate the decomposition of environmental pollutants, assess the risks and provide the storage conditions for energetic materials [34–36]. There are several methods to study the kinetics, including the isoconversional methods, the Kissinger method, the invariant kinetic parameters method, the model fitting methods, and the determination of reaction models and pre-exponential factors for model-free methods [37, 38]. The most common differential isoconversional method is that of Friedman [38]. In this study, the Friedman method was used to study the thermal degradation kinetics of photonically cured ECAs, hoping to provide helpful guidance for the fabrication and application of ECAs.

Experimental

Samples

In this study, the ECAs were composed of a matrix resin and electrically conductive fillers. The matrix resin was a Ripoxy SP-1507 vinyl ester resin from Showa Denko, Chibaken, Japan, which was a bisphenol A epoxy acrylate diluted by ethoxylated bisphenol A diacrylate. The viscosity was 18,700 mPa s (25 °C). The electrically conductive fillers were AgC-239 micro silver flakes (size 2–15 μm, thickness about 0.5 μm) from Fukuda Metal Foil & Powder Co., Ltd., Kyoto, Japan. The ECAs, containing 80 % of micro silver flakes by the mass, was named ECAs-80. To fabricate the ECAs, micro silver flakes were incorporated into the vinyl ester resin using a THINKY ARV-310 planetary vacuum mixer (THINKY Corporation, Laguna Hills, CA, USA.) with a mixing speed of 2,000 rpm for 20 min. After the fabrication, the ECAs were stored at room temperature for further use.

To prepare the cured products, the ECAs were printed into films (thickness 50 μm) on glass substrates. They were then photonically cured using a high-intensity Xenon flash lamp (PulseForge 3300 Photonic Curing System, Novacentrix, Austin, TX, USA.) under an ambient atmosphere at room temperature. 100 pulses were applied to cure the ECAs. The repetition rate was 3 Hz. The capacitor bank voltage was set at 220 V, the pulse duration was set to 1,400 μs, and the measured radiant exposure for each pulse was 2.4 J cm^{-2}.

Characterization

The thermal degradations of the samples were measured using a NETZSCH 2000SE/H/24/1 thermogravimetric analyzer (TGA, NETZSCH, Selb, Germany) operated under a pure N_2 atmosphere. The sample (ca. 10 mg) was placed in a Pt cell and heated at a rate of 5, 10, 15, and 20 °C min^{-1}, respectively, from 30 to 900 °C under a N_2 flow rate of 60 mL min^{-1}.

Results and discussion

Figure 1 presents the TG traces of photonically cured vinyl ester resin and ECAs-80. The mass loss began at about 300 °C and quickly increased from about 350–450 °C, where the thermal degradation rate was the maximum. Above that, the mass loss was slow. The thermal degradation temperature above 350 °C suggested the ECAs had high temperature stability. The mass curves were shifted to high temperature regions as heating rate increased from 5 to 10, 15, and 20 °C min^{-1}. Especially in the range of 350–450 °C, the shift was very clear. This is because high heating rate often caused a reaction hysteresis phenomenon and increased temperature gradients within the samples.

To investigate the thermal degradation kinetics, the thermal degradation processes between 300 and 500 °C were mainly focused. All kinetic studies can start with the basic equation, i.e., the rate of conversion equation, which relates to some function of the concentration of reactants. In this study, the ECAs matrix resin was a thermosetting resin, which also exhibited some thermosetting behavior, such as chemical structure and bonding strength [33]. For the thermosetting resins, the rate of conversion ($d\alpha/dt$) is usually expressed as [39, 40]:

$$\frac{d\alpha}{dt} = Ae^{-\frac{E}{RT}}f(\alpha), \tag{1}$$

where A and E are kinetic parameters, the pre-exponential factor and the activation energy, respectively, R is the universal gas constant, and T is the absolute temperature at time t.

Logarithmic Eq. (1) as:

$$\ln\left(\frac{d\alpha}{dt}\right) = -\frac{E}{RT} + \ln[Af(\alpha)] \tag{2}$$

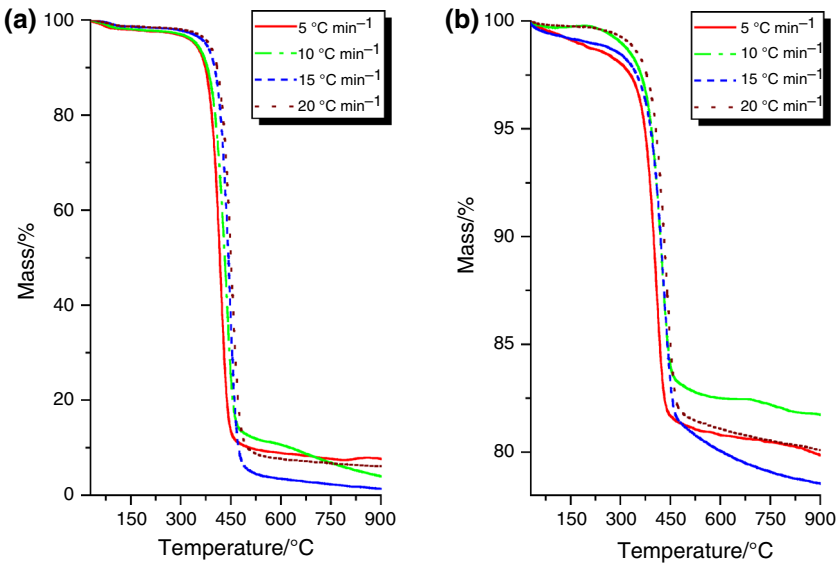

Fig. 1 TG traces of **a** vinyl ester resin and **b** ECAs-80 photonically cured under a radiant exposure energy of 2.4 J cm^{-2} per pulse for 100 pulses

In Eq. (2), α is the fractional extent conversion at a given time (or given temperature), expressed as:

$$\alpha = \frac{m_i - m_t}{m_i - m_f}, \tag{3}$$

where m_i is the mass of samples before thermal degradation, m_t is the mass of samples at time t during thermal degradation, and m_f is the mass of samples after thermal degradation (also called char yield).

Differentiating Eq. (3):

$$\frac{d\alpha}{dt} = -\frac{\frac{dm_t}{dt}}{m_i - m_f}, \tag{4}$$

where dm_t/dt is the thermal degradation rate, which can be obtained from the differential curves of mass curves in Fig. 1.

Because the thermal degradation of thermosetting resins also follows the kinetics of the mechanism of solid-state reactions [41], $f(\alpha)$, can be expressed as:

$$f(\alpha) = (1-\alpha)^n \alpha^m, \tag{5}$$

where $m + n$ is the overall order of reaction [42, 43].

From Eqs. (2) and (4), a plot of $\ln(d\alpha/dt)$ versus $1/T$ values at the same fractional extent of conversion α from a series of dynamic TG experiments at different heating rates will result in a straight line with a slope of $-E/R$ and an intercept of $\ln[Af(\alpha)]$. Repeating this procedure, the E and $\ln[Af(\alpha)]$ values corresponding to different α from the mass curves at different heating rates can be obtained. Thus, the relationship of E versus α and $\ln[Af(\alpha)]$ versus α can be determined. Simulating these relationships, the kinetic equations of the thermal degradation reaction can be obtained [38, 44].

Figure 2 is the plots of $\ln(d\alpha/dt)$ versus $1/T$ for photonically cured vinyl ester resin and ECAs-80 at various

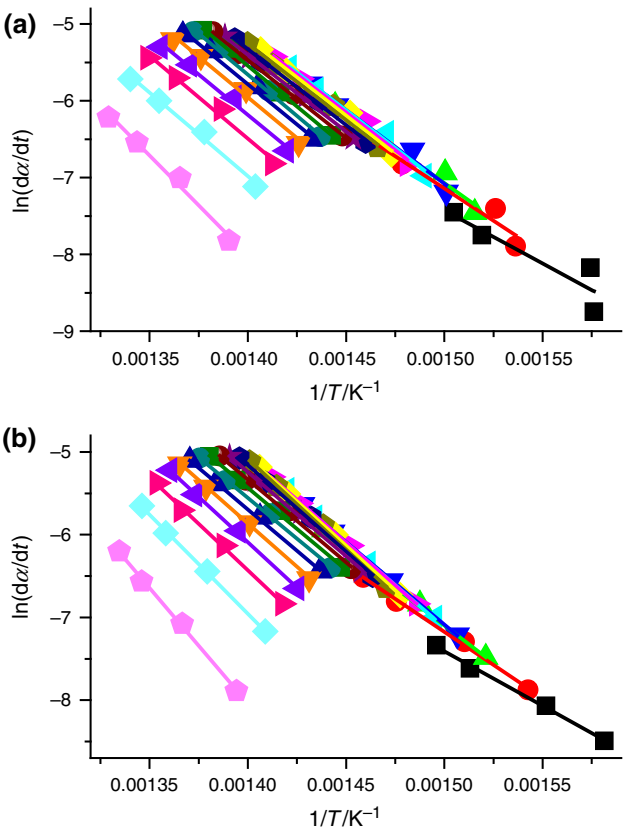

Fig. 2 Plots of $\ln(d\alpha/dt)$ versus $1/T$ for **a** vinyl ester resin and **b** ECAs-80 photonically cured under a radiant exposure energy of 2.4 J cm^{-2} per pulse for 100 pulses

values of α (α=0.05, 0.10, 0.15, 0.20, …, 0.90, 0.95) covering the experimental range. Making fitted linear regression lines, the groups of E and $\ln[Af(\alpha)]$ values were obtained for each value of α. Figure 3 shows the plots of

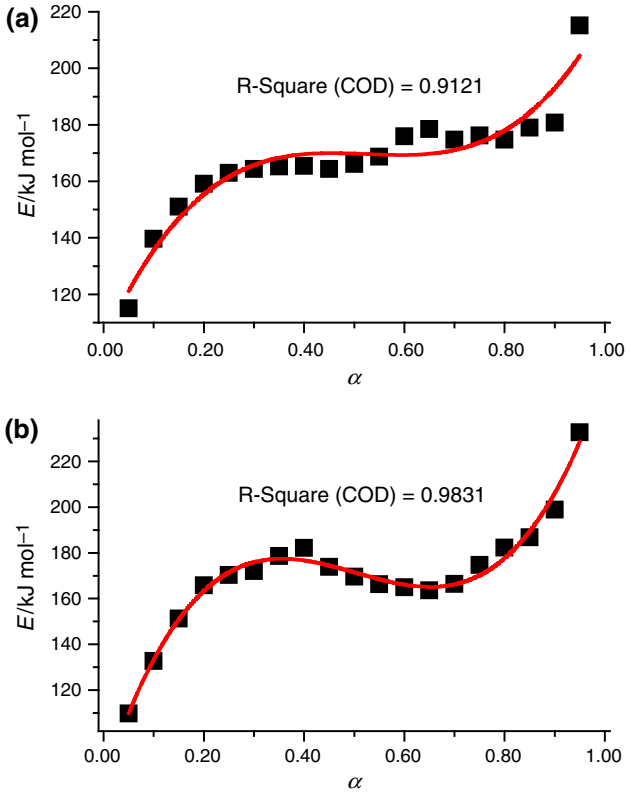

Fig. 3 Plots of E versus α for **a** vinyl ester resin and **b** ECAs-80 photonically cured under a radiant exposure energy of 2.4 J cm^{-2} per pulse for 100 pulses

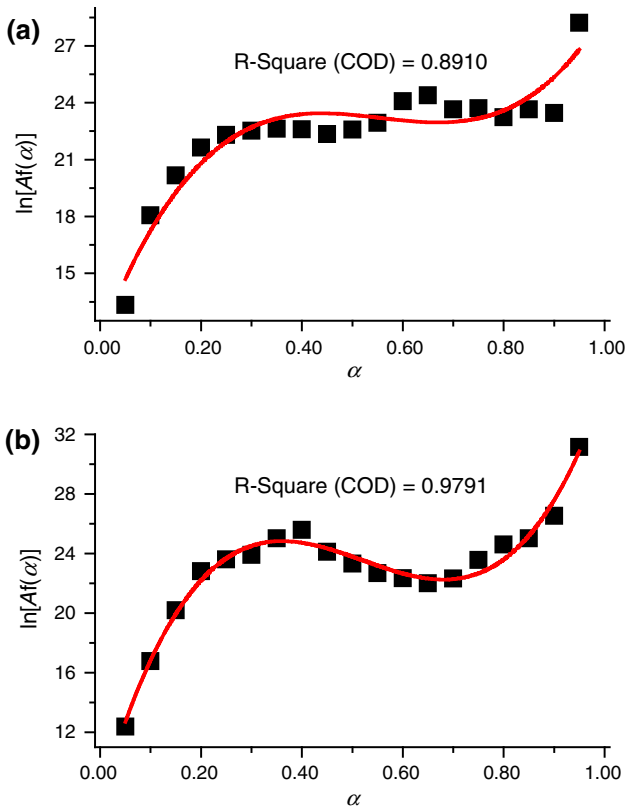

Fig. 4 Plots of ln[$Af(\alpha)$] versus α for **a** vinyl ester resin and **b** ECAs-80 photonically cured under a radiant exposure energy of 2.4 J cm^{-2} per pulse for 100 pulses

E versus α and Fig. 4 shows the plots of ln[$Af(\alpha)$] versus α, of photonically cured vinyl ester resin and ECAs-80. The different value of E corresponding to different α confirms the conversion-dependence of E. Trying different multiple regression equations to fit the data in Fig. 3, a cubic polynomial was found to be a good fit, i.e., if high-order moments were utilized to fit the data in Fig. 3, the coefficient of the items, whose number of order are greater than or equal to 4 in the equations, will be less than 10^{-5}, so cubic polynomial will suffice. The data in Fig. 4 were also fitted with a cubic polynomial achieving the required precision. As shown in Figs. 3 and 4, the fitted curves can represent dynamic TG results over a broad temperature range with a good fit.

Here, the photonically cured ECAs-80 was taken for an example to show the calculation of E, A, m, n, and $f(\alpha)$. Figures 1b, 2b, 3b, and 4b present the mass curves and plots of ln(dα/dt) versus $1/T$, E versus α, and ln[$Af(\alpha)$] versus α, respectively. The fitted multiple regression equations in Figs. 3b and 4b can be expressed as:

$$E(\alpha) = 961.73\alpha^3 - 1453.9\alpha^2 + 669.79\alpha + 79.859, \quad (6)$$

$$\ln[Af(\alpha)] = 158.71\alpha^3 - 248.02\alpha^2 + 117.05\alpha + 7.4366. \quad (7)$$

Substitute Eq. (5) into Eq. (7):

$$\ln A + n\ln(1-\alpha) + m\ln\alpha = 158.71\alpha^3 - 248.02\alpha^2 + 117.05\alpha + 7.4366 \quad (8)$$
$$\alpha \in (0,1).$$

To obtain more accurate m and n, here we let $\alpha = 0.05/0.50/0.90$, $0.10/0.50/0.90$, $0.15/0.50/0.85$, $0.20/0.50/0.80$, …, $0.40/0.50/0.60$, $0.45/0.50/0.55$, respectively. Taking $\alpha = 0.05/0.50/0.95$ for an example, an equation set with three variables can be obtained:

$$\ln A + n\ln 0.95 + m\ln 0.05 = 12.69, \quad (9)$$

$$\ln A + n\ln 0.50 + m\ln 0.50 = 23.80, \quad (10)$$

$$\ln A + n\ln 0.05 + m\ln 0.95 = 30.87 \quad (11)$$

Solving these equations yields the kinetic parameters: $m \approx 4.30$, $n \approx -1.87$, $\ln A \approx 25.48$.

Repeating this procedure for m and n values at $\alpha = 0.05/0.50/0.90$, $0.10/0.50/0.90$, $0.15/0.50/0.85$, $0.20/0.50/0.80$, …, $0.40/0.50/0.60$, $0.45/0.50/0.55$ (Table 1). In this study, the average values [45, 46] were used: $m = 1.85$ and $n = 2.22$, to calculate the kinetic equation of thermal degradation as follows:

Table 1 Calculated m, n, and ln$A$ for vinyl ester resin and ECAs-80 photonically cured under a radiant exposure energy of 2.4 J cm^{-2} per pulse for 100 pulses

α	Vinyl ester resin			ECAs-80		
	m	n	ln$A$	m	n	ln$A$
0.05/0.50/0.95	3.63	−0.49	25.53	4.30	−1.87	25.48
0.10/0.50/0.90	3.86	0.17	26.15	4.01	−0.89	25.96
0.15/0.50/0.85	3.79	0.89	26.60	3.33	0.30	26.31
0.20/0.50/0.80	3.60	1.59	26.96	2.52	1.50	26.58
0.25/0.50/0.75	3.36	2.23	27.23	1.70	2.62	26.79
0.30/0.50/0.70	3.12	2.78	27.45	0.96	3.60	26.96
0.35/0.50/0.65	2.91	3.23	27.61	0.35	4.40	27.09
0.40/0.50/0.60	2.75	3.55	27.73	−0.11	4.99	27.18
0.45/0.50/0.55	2.65	3.75	27.80	−0.40	5.35	27.23
Average	3.30	1.97	27.01	1.85	2.22	26.62

$$\frac{d\alpha}{dt} = e^{26.62}(1-\alpha)^{2.22}\alpha^{1.85}e^{-\frac{E(\alpha)}{RT}}, \tag{12}$$

with

$$E(\alpha) = 961.73\alpha^3 - 1453.9\alpha^2 + 669.79\alpha + 79.859 \quad \alpha \in (0,1). \tag{13}$$

Making the differential equation of $E(\alpha)$, viz. dE/dα:

$$\frac{dE}{d\alpha} = 2885.19\alpha^2 - 2907.8\alpha + 669.79 = 2885.19[(\alpha - 0.50)^2 - 0.15^2] \quad \alpha \in (0,1) \tag{14}$$

The E variations were expressed as the follows: $0 < \alpha < 0.35$, dE/d$\alpha > 0$; $\alpha = 0.35$, dE/d$\alpha = 0$; $0.35 < \alpha < 0.65$, dE/d$\alpha < 0$; $\alpha = 0.65$, dE/d$\alpha = 0$; $0.65 < \alpha < 1$, dE/d$\alpha > 0$ (Table 2).

Using the same method, the m, n, dα/dt, $E(\alpha)$, ln[$Af(\alpha)$], dE/dα, and E variations of photonically cured vinyl ester resin were calculated from the fitted multiple regression equations in Figs. 3a and 4a. They were listed in Tables 1 and 2 together with those of photonically cured ECAs-80. The kinetic equation of thermal degradation for photonically cured vinyl ester resin was:

$$\frac{d\alpha}{dt} = e^{27.01}(1-\alpha)^{1.97}\alpha^{3.30}e^{-\frac{E(\alpha)}{RT}} \tag{15}$$

with

$$E(\alpha) = 488.07\alpha^3 - 766.8\alpha^2 + 394.47\alpha + 103.28 \quad \alpha \in (0,1) \tag{16}$$

The differential equation of $E(\alpha)$, viz. dE/dα:

$$\frac{dE}{d\alpha} = 1464.21\alpha^2 - 1533.6\alpha + 394.47 = 1464.21[(\alpha - 0.52)^2 - 0.07^2] \quad \alpha \in (0,1), \tag{17}$$

which showed E variations: $0 < \alpha < 0.45$, dE/d$\alpha > 0$; $\alpha = 0.45$, dE/d$\alpha = 0$; $0.45 < \alpha < 0.59$, dE/d$\alpha < 0$; $\alpha = 0.59$, dE/d$\alpha = 0$; $0.59 < \alpha < 1$, dE/d$\alpha > 0$.

Figure 3b shows E versus α of photonically cured ECAs-80. The fitted multiple regression line presented the variations of E clearly. The value of E spanned from 110 to 233 kJ mol^{-1}. During the thermal degradation, the value of E first increased at $0 < \alpha < 0.35$, and reached a maximum value of 177 kJ mol^{-1} at $\alpha = 0.35$. Then it decreased at $0.35 < \alpha < 0.65$, and reached a minimum value of 164 kJ mol^{-1} at $\alpha = 0.65$. Finally, the value of E increased again at $0.65 < \alpha < 1$ as the thermal degradation further progressed. This may be related to the crosslinked network structures by photonic curing [33]. In the initial heating stage, it is difficult to decompose and volatilize these crosslinked network structures, so E increased at low conversions ($0 < \alpha < 0.35$) and reached a maximum value at 177 kJ mol^{-1} when $\alpha = 0.35$. As the temperature rose continually from 350 to 450 °C (Fig. 1b), thermal

Table 2 Thermal degradation kinetics of vinyl ester resin and ECAs-80, photonically cured under a radiant exposure energy of 2.4 J cm^{-2} per pulse for 100 pulses

	Vinyl ester resin	ECAs-80
dα/dt	$e^{27.01}(1-\alpha)^{1.97}\alpha^{3.30}e^{-\frac{E(\alpha)}{RT}}$ $\alpha \in (0,1)$	$e^{26.62}(1-\alpha)^{2.22}\alpha^{1.85}e^{-\frac{E(\alpha)}{RT}}$ $\alpha \in (0,1)$
ln[$Af(\alpha)$]	$78.397\alpha^3 - 130.46\alpha^2 + 69.246\alpha + 11.552$ $\alpha \in (0,1)$	$158.71\alpha^3 - 248.02\alpha^2 + 117.05\alpha + 7.4366$ $\alpha \in (0,1)$
E	$488.07\alpha^3 - 766.8\alpha^2 + 394.47\alpha + 103.28$ $\alpha \in (0,1)$	$961.73\alpha^3 - 1453.9\alpha^2 + 669.79\alpha + 79.859$ $\alpha \in (0,1)$
dE/dα	$1464.21\alpha^2 - 1533.6\alpha + 394.47$ $\alpha \in (0,1)$	$2885.19\alpha^2 - 2907.8\alpha + 669.79$ $\alpha \in (0,1)$
dE/dα Variation	$0 < \alpha < 0.45$, dE/d$\alpha > 0$; $\alpha = 0.45$, dE/d$\alpha = 0$; $0.45 < \alpha < 0.59$, dE/d$\alpha < 0$; $\alpha = 0.59$, dE/d$\alpha = 0$; $0.59 < \alpha < 1$, dE/d$\alpha > 0$.	$0 < \alpha < 0.35$, dE/d$\alpha > 0$; $\alpha = 0.35$, dE/d$\alpha = 0$; $0.35 < \alpha < 0.65$, dE/d$\alpha < 0$; $\alpha = 0.65$, dE/d$\alpha = 0$; $0.65 < \alpha < 1$, dE/d$\alpha > 0$.
ln$A$	27.01	26.62
$m + n$	5.27	4.07
m	3.30	1.85
n	1.97	2.22

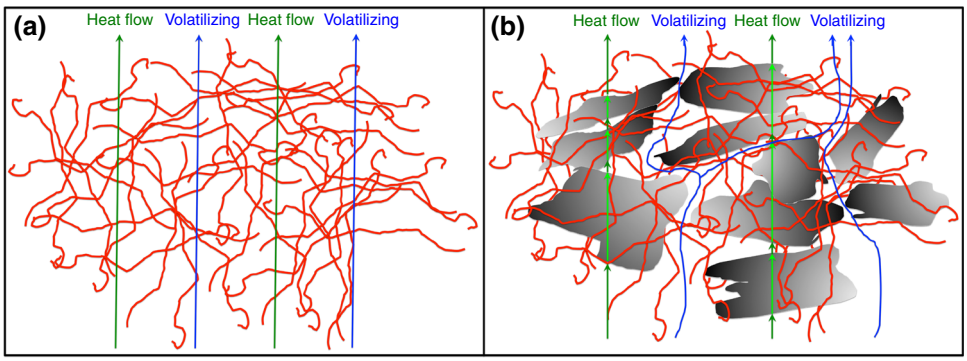

Fig. 5 Heat flows and volatilizing in **a** vinyl ester resin and **b** ECAs-80 photonically cured under a radiant exposure energy of 2.4 J cm^{-2} per pulse for 100 pulses

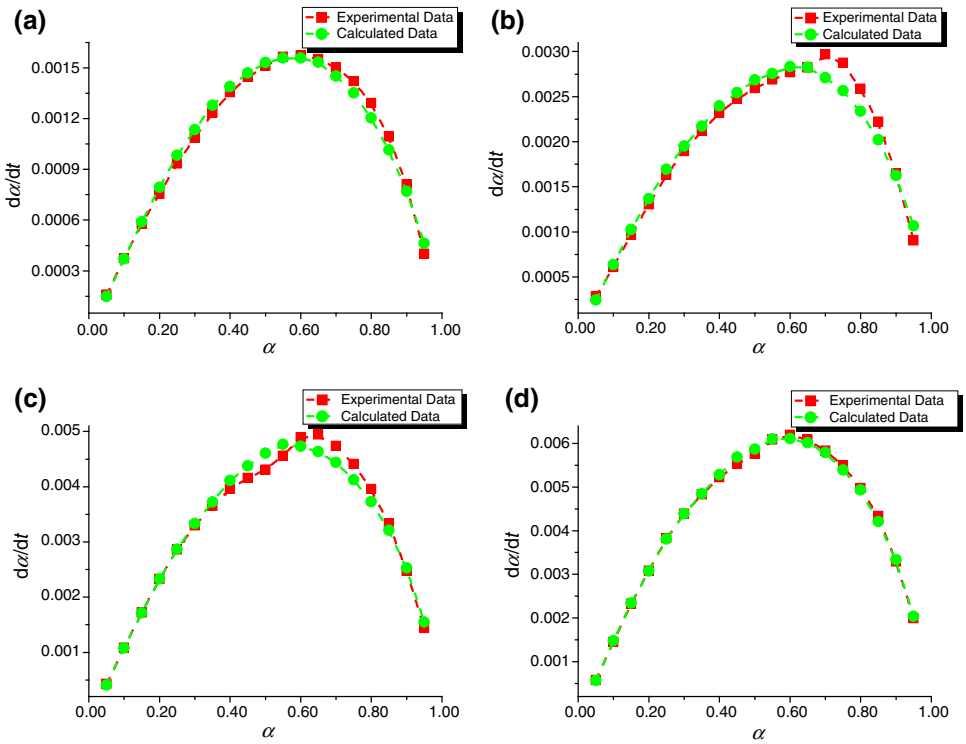

Fig. 6 Comparisons of experimental data with the kinetic method results of photonically cured vinyl ester resin at curing rates of **a** 5 °C min^{-1}, **b** 10 °C min^{-1}, **c** 15 °C min^{-1}, and **d** 20 °C min^{-1}

degradation mainly occurred for these crosslinked network structures to decompose into low molecular substances. As the thermal degradation reaction progressed more easily, these low molecular substances were decomposed and volatilized at high temperatures. Therefore, E decreased at medium conversions ($0.35 < \alpha < 0.65$) and reached a minimum value at 164 kJ mol^{-1} when $\alpha = 0.65$. In the final heating stage, because the crosslinked network structures were destroyed completely and the low molecular substances were decomposed fully, only thermal degradation residues were left. They contained aromatic compounds, which were also difficult to decompose and volatilize, so E increased again at high conversions ($0.65 < \alpha < 1$). In this study, the minimum value of 164 kJ mol^{-1} ($\alpha = 0.65$) was used as the activation energy for the thermal degradation of photonically cured ECAs-80, because the minimum value is always closer to the "real" activation energy [38, 41, 42, 44].

Because of the same reasons mentioned above, photonically cured vinyl ester resin showed similar E variations as photonically cured ECAs-80. Figure 3a shows E versus α and the fitted multiple regression lines of photonically cured vinyl ester resin. E spanned from 115 to 215 kJ mol^{-1}. As the thermal degradation progressed, the E first increased to a maximum value of 170 kJ mol^{-1} at $\alpha = 0.45$, then decreased to a minimum value of 169 kJ mol^{-1} at $\alpha = 0.59$, subsequently, E increased again. In this study, the minimum value of 169 kJ mol^{-1} at $\alpha = 0.59$ was used as the activation energy for the thermal degradation of photonically cured vinyl ester resin.

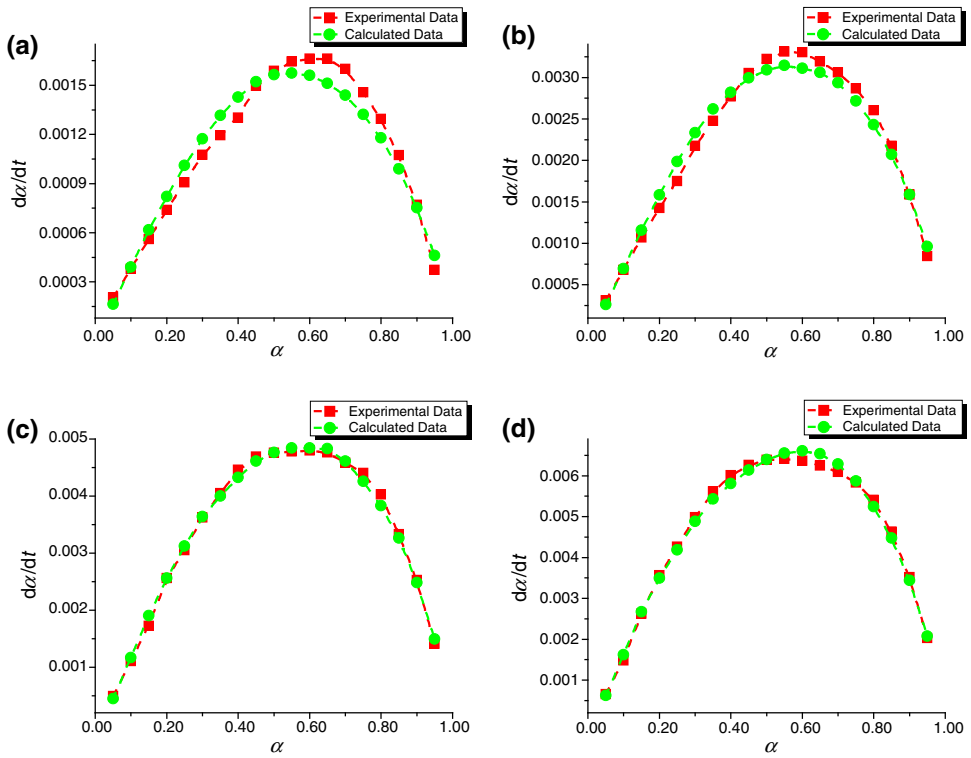

Fig. 7 Comparisons of experimental data with the kinetic method results of photonically cured ECAs-80 at curing rates of **a** 5 °C min^{-1}, **b** 10 °C min^{-1}, **c** 15 °C min^{-1}, and **d** 20 °C min^{-1}

Apparently, photonically cured vinyl ester resin and ECAs-80 had similar, or even identical, variations of E, which both showed increasing–decreasing–increasing variation trends presumably due to the inclusion of the same vinyl ester resin that determined the thermal degradation.

However, there were some differences between the variations of E of photonically cured vinyl ester resin and ECAs-80. During the thermal degradation of photonically cured vinyl ester resin, the heat transferred between/among the thermosetting polymers and passed through the crosslinked network structures (Fig. 5a). In the case of ECAs-80, micro silver flakes were the electrically conductive fillers, which were excellent thermal conductors (thermal conductivity 429 W m^{-1} K^{-1}). During the thermal degradation, the micro silver flakes formed many new thermally conductive channels (Fig. 5b). This process increased the transfer rate of heat, improved the decomposition rate, and accelerated the thermal degradation. Therefore, photonically cured ECAs-80 reached the maximum value of 177 kJ mol^{-1} at $\alpha = 0.35$ (Fig. 3b). This was earlier than that of photonically cured vinyl ester resin at 170 kJ mol^{-1} at $\alpha = 0.45$ (Fig. 3a), and suggested that the crosslinked network structures in photonically cured ECAs-80 can be destroyed more quickly than in photonically cured vinyl ester resin at high temperatures.

During thermal degradation, polymers are always decomposed into small molecules which are taken away by the gas stream. This process is called volatilization. In this study, the crosslinked network structures were destroyed and decomposed into low molecular substances. As the temperature rose and the thermal degradation continued to progress, these low molecular substances were further decomposed and volatilized gradually. In photonically cured vinyl ester resin, they were volatilized easily without any impediment to escape (Fig. 5a). In contrast, micro silver flakes blocked the volatilization in photonically cured ECAs-80. This is because they can transfer heat, but they cannot transfer mass. As Fig. 5b shows, the volatilization was not like that of heat flow. The volatilization products had to take a circuitous route around the micro silver flakes in order to escape and be swept away by the gas stream. In other words, micro silver flakes lengthened or delayed the volatilization processes; photonically cured ECAs-80 needed a longer time to volatilize all of the decomposed small molecules than photonically cured vinyl ester resin at high temperatures. It can be seen that photonically cured ECAs-80 reached the minimum value of 164 kJ mol^{-1} when $\alpha = 0.65$ (Fig. 3b) later than that of photonically cured vinyl ester resin at 169 kJ mol^{-1} as $\alpha = 0.59$ (Fig. 3a).

Moreover, A and $m + n$ also reflected the variations of E. In the thermal degradation kinetics, A is a constant determined by the reaction essence. It does not have any relationship to the reaction temperatures and concentrations in the system. In this study, the minimum values of 169 kJ mol^{-1} ($\alpha = 0.59$) and 164 kJ mol^{-1} ($\alpha = 0.65$)

were used as the activation energies for the thermal degradation of photonically cured vinyl ester resin and ECAs-80, respectively. A changed accordingly with E [47, 48]: photonically cured ECAs-80 presented a lower A value at $e^{26.62}$ than that of photonically cured vinyl ester resin at $e^{27.01}$ (Table 2). Similarly, photonically cured ECAs-80 also presented a lower $m + n$ at 4.07 than that of photonically cured vinyl ester resin at 5.27. The $m + n > 1$ demonstrated that the thermal degradations of photonically cured vinyl ester resin and ECAs-80 were complex, which were also proved by the E variations during the whole thermal degradation.

To demonstrate the applicability of the Friedman method, the results calculated from this kinetic method were compared with those from experiments, as shown in Figs. 6 and 7. Here, the experimental data were from Eq. (4), the calculated data from the kinetic equations of photonically cured vinyl ester resin [Eq. (15)] and ECAs-80 [Eq. (12)]. It can be seen that they were in good agreements with each other. In addition, the differences between model predictions and experimental data were also observed when the heating rate increased. The experimental and calculated data of 5, 10, and 15 °C min^{-1} heating rates presented apparent divergences at medium conversions for photonically cured vinyl ester resin (Fig. 6a, b, and c), as photonically cured ECAs-80 did at 5 and 10 °C min^{-1} heating rates (Fig. 7a and 7b). The neglect of diffusion factor as the kinetic method was deduced may be responsible for the deviations between experimental and calculated data [49, 50]. The calculated data displayed good agreements with experimental data for photonically cured vinyl ester resin at 20 °C min^{-1} heating rate (Fig. 6d) and photonically cured ECAs-80 at 15 and 20 °C min^{-1} heating rates (Fig. 7c and d) in the whole tested conversion range. The better degree of agreements of kinetic method results with experimental data at higher heating rates, indicating the temperature dependence of the diffusion and reaction rate. For the dynamic TG, the higher the heating rate, the higher the temperature range of the thermal degradation occurred.

Conclusions

In this study, the thermal degradation kinetics of high-intensity pulsed light cured ECAs fabricated from vinyl ester resin and micro silver flakes was studied using the Friedman method and deduced by assuming a variable E. The value of E spanned from 110 to 233 kJ mol^{-1}, which first increased, then decreased, and finally increased again as the thermal degradation proceeded. The kinetic equation of thermal degradation was obtained at $d\alpha/dt = e^{26.62}(1-\alpha)^{2.22}\alpha^{1.85}e^{(-E(\alpha)/RT)}$ with $E(\alpha) = 961.73\alpha^3 - 1453.9\alpha^2 + 669.79\alpha + 79.859$, $\alpha \in (0,1)$. The $m + n$ was 4.07 and >1, which demonstrated that the thermal degradation of photonically cured ECAs was complex. With the Friedman method, we can have a comprehensive and in-depth understanding of the thermal degradation kinetics of photonically cured ECAs.

References

1. Liu J. Conductive adhesives for electronics packaging. Isle of Man: Electrochemical Publications Ltd.; 1999.
2. Suhir E, Lee YC, Wong CP. Micro- and opto-electronic materials and structures: physics, mechanics, design, reliability, and packaging. New York: Springer; 2007.
3. Liu J, Salmela O, Sarkka J, Morris JE, Tegehall PE, Andersson C. Reliability of microtechnology: interconnects, devices and systems. New York: Springer; 2011.
4. Cui HW, Fan Q, Li DS, Tang X. Formulation and characterization of electrically conductive adhesives for electronic package. J Adhes. 2013;89:19–36.
5. Cui HW, Du WH. Novel fast curing electrically conductive adhesives from a functional epoxy and micro silver flakes: preparation, characterization, and humid-thermal aging. J Adhes. 2013;89:714–26.
6. Cui HW, Li DS, Fan Q. Reliability of flexible electrically conductive adhesives. Polym Adv Technol. 2013;24:114–7.
7. Inoue M, Muta H, Yamanaka S, Suganuma K. Electrical properties of isotropic conductive adhesives composed of silicone-based elastomer binders containing Ag particles. J Electron Mater. 2009;38:2013–22.
8. Li Z, Hansen K, Yao YG, Ma YQ, Moon KS, Wong CP. The conduction development mechanism of silicone-based electrically conductive adhesives. J Mater Chem C. 2013;1:4368–74.
9. Yoonessi M, Scheiman DA, Dittler M, Peck JA, Ilavskye J, Gaierc JR. Meador MA. High-temperature multifunctional magnetoactive nickel graphene polyimide nanocomposites. Polymer. 2013;54:2776–84.
10. Zhong XH, Wang R, Wen YY. Effective reinforcement of electrical conductivity and strength of carbon nanotube fibers by silver-paste-liquid infiltration processing. Phys Chem Chem Phys. 2013;15:3861–5.
11. Yin Q, Li AJ, Wang WQ, Xia LG, Wang YM. Study on the electrical and mechanical properties of phenol formaldehyde resin/graphite composite for bipolar plate. J Power Sources. 2007;165:717–21.
12. Liu NL, Qi SH, Li SS, Wu XM, Wu LM. Preparation and characterization of phenol formaldehyde/Ag/graphite nanosheet composites. Polym Test. 2011;30:390–6.
13. Araki T, Nogi M, Suganuma K, Kogure M, Kirihara O. Printable and stretchable conductive wirings comprising silver flakes and elastomer. IEEE Electron Device Lett. 2011;32:1424–6.
14. Araki T, Sugahara T, Nogi M, Suganuma K. Effect of void volume and silver loading on strain response of electrical resistance in silver flakes/polyurethane composite for stretchable conductors. Jpn J Appl Phys. 2012;51:11PD01.
15. Abderrahmen R, Gavory C, Chaussy D, Briançon S, Fessi H, Belgacem MN. Industrial pressure sensitive adhesives suitable for physicochemical microencapsulation. Int J Adhes Adhes. 2011;31:629–33.
16. Czech Z, Kowalczyk A, Pełech R, Wróbelb RJ, Shao L, Bai Y, Świdersk J. Using of carbon nanotubes and nano carbon black for electrical conductivity adjustment of pressure-sensitive adhesives. Int J Adhes Adhes. 2012;36:20–4.

17. Ho LN, Nishikawa H. Surfactant-free synthesis of copper particles for electrically conductive adhesive applications. J Electron Mater. 2012;41:2527–32.
18. Zhu XY, Liu YL, Long JM, Liu XL. Electrochemical migration behavior of Ag-plated Cu-filled electrically conductive adhesives. Rare Met. 2012;31:64–70.
19. Tan FT, Qiao XL, Chen JG, Wang HS. Effects of coupling agents on the properties of epoxy-based electrically conductive adhesives. Int J Adhes Adhes. 2006;26:406–13.
20. Cui HW, Fan Q, Li DS. Novel flexible electrically conductive adhesives from functional epoxy, flexibilizers, micro silver flakes and nano silver spheres for electronic package. Polym Int. 2013;62:1644–51.
21. Yang XJ, He W, Wang SX, Zhou GY, Tang Y. Preparation and properties of a novel electrically conductive adhesive using a composite of silver nanorods, silver nanoparticles, and modified epoxy resin. J Mater Sci-Mater Electron. 2012;23:108–14.
22. Si GY, Zhao YH, Lv JT, Lu MQ, Wang FW, Liu HL, Xiang N, Huang TJ, Danner AJ, Teng JH, Liu YJ. Reflective plasmonic color filters based on lithographically patterned silver nanorod arrays. Nanoscale. 2013;5:6243–8.
23. Kwon Y, Yim BS, Kim JM, Kim J. Dispersion, hybrid interconnection and heat dissipation properties of functionalized carbon nanotubes in epoxy composites for electrically conductive adhesives (ECAs). Microelectron Reliab. 2011;51:812–8.
24. Cui HW, Kowalczyk A, Li DS, Fan Q. High performance electrically conductive adhesives from functional epoxy, micron silver flakes, micron silver spheres and acidified single wall carbon nanotube for electronic package. Int J Adhes Adhes. 2013; 44:220–5.
25. Cui HW, Li DS, Fan Q. Using a functional epoxy, micron silver flakes, nano silver spheres, and treated single-wall carbon nanotubes to prepare high performance electrically conductive adhesives. Electron Mater Lett. 2013;9:299–307.
26. Zhang Y, Qi SH, Wu XM, Duan GC. Electrically conductive adhesive based on acrylate resin filled with silver plating graphite nanosheet. Synth Met. 2011;161:516–22.
27. Tang J, Chen Q, Xu LG, Zhang S, Feng LZ, Cheng L, Xu H, Liu Z, Peng R. Graphene oxide-silver nanocomposite as a highly effective antibacterial agent with species-specific mechanisms. ACS Appl Mater Interfaces. 2013;5:3867–74.
28. Zhang ZX, Chen XY, Xiao F. The sintering behavior of electrically conductive adhesives filled with surface modified silver nanowires. J Adhes Sci Technol. 2011;25:1465–80.
29. Jiu JT, Nogi M, Sugahara T, Tokuno T, Araki T, Komoda N, Suganuma K, Uchida H, Shinozaki K. Strongly adhesive and flexible transparent silver nanowire conductive film fabricated with high-intensity pulsed light technique. J Mater Chem. 2012;22:23561–7.
30. Cui HW, Li DS, Fan Q. Using nano hexagonal boron nitride particles and nano cubic silicon carbide particles to improve the thermal conductivity of electrically conductive adhesives. Electron Mater Lett. 2013;9:1–5.
31. Cui HW, Li DS, Fan Q, Lai HX. Electrical and mechanical properties of electrically conductive adhesives from epoxy, micro-silver flakes, and nano-hexagonal boron nitride particles after humid and thermal aging. Int J Adhes Adhes. 2013; 44:232–6.
32. Cui HW, Tang X. Using polyurethane, ethylene-vinyl acetate hotmelt, and nano hexagonal boron nitride particles to electrospin high surface adhesion polymer fibers. Electron Mater Lett. 2014;10:183–9.
33. Cui HW, Jiu JT, Nagao S, Sugahara T, Suganuma K, Uchida H, Schroder KA. Ultra-fast photonic curing electrically conductive adhesives from vinyl ester resin and silver flakes. RSC Adv. 2014;4:15914–22.
34. Wang XJ, Wu JQ, Li YM, Zhou CJ, Xu CH. Pyrolysis kinetics and pathway of polysiloxane conversion to an amorphous SiOC ceramic. J Therm Anal Calorim. 2014;115:55–62.
35. Carmona VB, de Campos A, Marconcini JM, Mattoso LHC. Kinetics of thermal degradation applied to biocomposites with TPS, PCL and sisal fibers by non-isothermal procedures. J Therm Anal Calorim. 2014;115:153–60.
36. Kunzel M, Yan QL, Selesovsky J, Zeman S, Matyas R. Thermal behavior and decomposition kinetics of ETN and its mixtures with PETN and RDX. J Therm Anal Calorim. 2014;115:289–99.
37. Chandran K, Kamruddin M, Muralidaran P, Ganesan V. Thermal decomposition of sodium propoxides Kinetic studies using model-free method under isothermal and non-isothermal conditions. J Therm Anal Calorim. 2013;112:63–71.
38. Mothe CG, de Miranda IC. Study of kinetic parameters of thermal decomposition of bagasse and sugarcane straw using Friedman and Ozawa-Flynn-Wall isoconversional methods. J Therm Anal Calorim. 2013;112:497–505.
39. Kozlov A, Svishchev D, Donskoy I, Keiko AV. Thermal analysis in numerical thermodynamic modeling of solid fuel conversion. J Therm Anal Calorim. 2012;109:1311–7.
40. Nassar NN, Hassan A, Luna G, Pereira-Almao P. Comparative study on thermal cracking of Athabasca bitumen Evaluation of the activation energy and prediction of the isothermal conversion by different isoconversional methods. J Therm Anal Calorim. 2013;114:465–72.
41. Galwey AK. Theory of solid-state thermal decomposition reactions. J Therm Anal Calorim. 2012;109:1625–35.
42. Kamal MR, Sourour S. Kinetics and thermal characterization of thermoset cure. Polym Eng Sci. 1973;13:59–64.
43. Wendlandt WW. Thermal analysis. New York: Wiley-Blackwell; 1986.
44. Flynn JH. A general differential technique for the determination of parameters for $d\alpha/dt = f(\alpha)A\exp(-E/RT)$. J Therm Anal. 1991;37:293–305.
45. Hu RZ, Shi QZ. Thermal analysis kinetics. Beijing: Science Press; 2001.
46. Cui HW, Jiu JT, Nagao S, Sugahara T, Suganuma K, Uchida H. Using Ozawa method to study the curing kinetics of electrically conductive adhesives. J Therm Anal Calorim. 2014;117:1365–73.
47. Han YQ, Li TX, Saito K. A modified Ortega method to evaluate the activation energies of solid state reactions. J Therm Anal Calorim. 2013;112:683–7.
48. Gallego J, Batiot-Dupeyat C, Mondragon F. Activation energies and structural changes in carbon nanotubes during different acid treatments. J Therm Anal Calorim. 2013;114:597–602.
49. Ortiz-Landeros J, Avalos-Rendon TL, Gomez-Yanez C, Pfeiffer H. Analysis and perspectives concerning CO2 chemisorption on lithium ceramics using thermal analysis. J Therm Anal Calorim. 2012;108:647–55.
50. Saad GR, Eldin AFS. Isothermal cure kinetics of uncatalyzed and catalyzed diglycidyl ether of bisphenol-A/carboxylated polyester hybrid powder coating. J Therm Anal Calorim. 2012; 110:1425–30.